

Studies of Proximity Focusing RICH with an aerogel radiator using Flat-panel multi-anode PMTs (Hamamatsu H8500)

T. Matsumoto^{a,*} S. Korpar^b I. Adachi^c S. Fratina^b T. Iijima^d
R. Ishibashi^e H. Kawai^e P. Križan^b S. Ogawa^f R. Pestotnik^b
S. Saitoh^c T. Seki^a T. Sumiyoshi^a K. Suzuki^c T. Tabata^e
Y. Uchida^f Y. Unno^e

^a*Tokyo Metropolitan University, Tokyo, Japan*

^b*Jožef Stefan Institute, Ljubljana, Slovenia*

^c*High Energy Accelerator Research Organization (KEK), Tsukuba, Japan*

^d*Nagoya University, Nagoya, Japan*

^e*Chiba University, Chiba, Japan*

^f*Toho University, Funabashi, Japan*

Abstract

A proximity focusing ring imaging Cherenkov detector using aerogel as the radiator has been studied for an upgrade of the Belle detector at the KEK-B-factory. We constructed a prototype Cherenkov counter using a 4×4 array of 64-channel flat-panel multi-anode PMTs (Hamamatsu H8500) with a large effective area. The aerogel samples were made with a new technique to obtain a higher transmission length at a high refractive index ($n = 1.05$). Multi-channel PMTs are read-out with analog memory chips. The detector was tested at the KEK-PS $\pi 2$ beam line in November, 2002. To evaluate systematically the performance of the detector, tests were carried out with various aerogel samples using pion beams with momenta between 0.5 GeV/ c and 4 GeV/ c . The typical angular resolution was around 14 mrad, and the average number of detected photoelectrons was around 6. We expect that pions and kaons can be separated at a 4σ level at 4 GeV/ c .

Key words: Aerogel, Flat-panel PMT, Ring Imaging Cherenkov Counter, Proximity Focusing, Particle Identification, Belle

PACS: 29.40.Ka

* Corresponding author. Tel: +81-426-77-2500; fax: +81-426-77-2483
Email address: matumot@bmail.kek.jp (T. Matsumoto).

1 Introduction

Silica aerogel is a unique material with a refractive index (n) in the range between gases and liquids or solids. Its refractive index can be easily controlled from $n = 1.01$ to 1.06 . As a result, the refractive index of the aerogel can be chosen such that for a given momentum interval in the few GeV/ c region charged pions radiate Cherenkov photons, while kaons stay below the Cherenkov radiation threshold [1]. In the Belle experiment at KEK [2], a threshold type Cherenkov detector (Belle-ACC) [3] which uses aerogel as a radiator, is operated, providing at 3.5 GeV/ c a kaon identification efficiency of 88% with a pion misidentification probability of 8% [4].

A new production method of hydrophobic aerogel with a high transmission length and n in the interval between 1.01 and 1.03 was developed during the construction period of Belle-ACC [5]. The improvement in quality allows the use of an aerogel radiator in a ring imaging Cherenkov counter (RICH) [6]. In the HERMES experiment at DESY, a RICH counter is used with a dual-radiator (aerogel and gas), and mirrors to focus the Cherenkov photons [7]. A similar detector is also designed for the LHCb experiment at CERN [8].

We are studying the feasibility of a RICH counter with an aerogel radiator for the Belle-ACC in the forward end-cap region [9]. Since this part is now optimized for the pion/kaon separation needed for tagging of the B flavor, and covering the momentum range below 2 GeV/ c , separation at high-momentum region of around 4 GeV/ c is not adequate. This kinematic region is, however, very important for the studies of two-body decays such as $B \rightarrow \pi\pi$, $K\pi$. In order to achieve a π/K separation for a wider momentum range, a ring imaging-type of detector is needed. Due to spatial restrictions, such a counter has to be of the proximity focusing type. To cover the identification in the lower momentum region (around 0.7 GeV/ c) as well as in the region up to 4 GeV/ c , the aerogel has to have a refractive index around $n = 1.05$. The first beam test of such a detector was carried out in 2001 at the KEK-PS π^2 beam line [10]. These tests used an array of multi-anode PMTs (Hamamatsu R5900-M16) for photo-detection. The detected number of photoelectrons was 2.7 per ring for a 2 cm thick aerogel tile with $n = 1.05$, and the Cherenkov angle resolution per photon was 10 mrad. These results were consistent with expectations. The number of detected photons was, however, rather low, partly because only 36% of the detector surface was covered by the photo-cathodes, and partly because the transmission length of the aerogel with $n = 1.05$ could not be made large enough. For the second beam test, we improved the aerogel transmission by optimizing the materials used in the production process. The active area fraction of the photon detector was increased by employing recently developed flat-panel PMTs, Hamamatsu H8500. Although this type of PMT is not immune to magnetic field, and therefore cannot be applied in

the Belle spectrometer, we consider this device as an intermediate step in our development. The paper is organized as follows. We first present the experimental set-up with flat-panel PMTs, briefly review the improvement in aerogel production, describe the measurements, and finally discuss the results.

2 The experiment set-up

2.1 Flat-panel PMT

The photon detector for the tested prototype RICH counter employed 64 channel multi-anode PMTs (Hamamatsu H8500, so called flat-panel PMT) because of their large effective area. 16 PMTs were used in a 4×4 array and aligned with a 52.5 mm pitch, as shown in Figure 1. The surface of each PMT is divided into 64 (8×8) channels with a 6.0×6.0 mm² pixel size. Therefore, the effective area of photon detection is increased to 84%. At the back of each PMT, an analog memory board is attached to read out multi-channel PMT signals, as described below. Among 16 PMTs, 8 PMTs were delivered in January, 2002, and the remaining PMTs were delivered in October, 2002. Since the manufacture method of the PMT was still under development, they exhibit a large variation in quantum efficiency and gain. The quantum efficiency at 400 nm varies between 16% and 25%; the gain varies from $1 \cdot 10^6$ to $6 \cdot 10^6$ when the maximal allowed high voltage of -1100 V is applied to the photo-cathode [11]. The PMTs from the later batch show a slightly better performance.

2.2 Aerogel radiator

The hydrophobic form of the aerogel radiator from Novosibirsk [13] is known to have a long transmission length. However we prefer hydrophobic aerogel than hydrophilic one for the application to a collider experiment. With a low refractive index ($n = 1.01 \sim 1.03$), such an aerogel was developed for the Belle-ACC, and is characterized by a high transmission length (~ 40 mm at a wave length of 400 nm) which was not achieved before. However, the transmission length of aerogel with a higher refractive index of $n = 1.05$ fell below one half the value compared to the aerogel with $n = 1.03$. Therefore, we reexamined the aerogel production technique in a joint development with Matsushita Electric Works Ltd. As a result, we found that the important factors determining the transmission length are the solvent and selection of the precursor to be used for its production. Originally, we used methyl-alcohol for the solvent, and methyl-silicate as a precursor [5]. When we applied di-

methyl-formamide (DMF) [12], and changed the supplier of the precursor, we could improve the transmission length of the aerogel.

Figure 2 shows the refractive indices of aerogel and the relation to transmission length for samples which were used in this beam test. The refractive index was determined by measuring the deflection angle of laser light (laser diode: 405 nm) at a corner of each aerogel tile; the transmission length was measured with a photo-spectrometer (Hitachi U-3210). In addition to the samples produced with the new technique at Matsushita Electric Works Ltd. and Chiba university, samples from BINP (Novosibirsk) were tested [13]; for comparison, we also tested the samples used in the previous beam test. The thicknesses of the prepared aerogel samples ranged from 10 mm to 25 mm. Various thickness of up to about 50 mm were tested by stacking these samples. Note that in the production of the aerogel samples at BINP propenol was used as the solvent, and the resulting aerogel was hydrophilic. Also note that the Matsushita aerogel samples produced with the new technique have a very similar transmission length as the BINP samples. The transmission length for $n \sim 1.05$ samples used in the first beam test was around 15 mm, but was increased to 45 mm for Matsushita's sample with the new production method.

2.3 Beam set-up

For the beam test, pions with momenta between 0.5 GeV/ c and 4 GeV/ c were used. Beside the RICH detector under study, counters for triggering, tracking and particle identification were employed.

The set up of the aerogel RICH is shown in Figure 3. Two RICH counters were placed in a light-shield box and tested simultaneously. Each RICH was composed of a layer of aerogel radiator and a photo-detection plane, parallel to the radiator face at a distance of 20 cm. The upstream Cherenkov counter was the detector under study; the downstream counter was the one employed in the previous beam test. Since the latter uses a well-known photo-detector, multi-anode PMTs Hamamatsu R5900, we regarded it as a reference.

Particle identification was done to remove particles other than pions. Two CO₂ gas Cherenkov counters in the beam line were used to exclude electrons. Also, an aerogel counter was equipped and used to exclude protons for the high-momentum region. This detector was also used to exclude muons for the low-momentum region around 0.5 GeV/ c .

The particle trajectories were measured with multi-wire proportional chambers (MWPC) at the upstream and downstream ends of the light-shield box. These 5×5 cm² MWPCs, with 20 μ m diameter, gold-plated tungsten anode wires at 2 mm pitch and with 90% Ar + 10% CH₄ gas flow, were read out by

delay lines on the x and y cathode strips.

The trigger signal was generated as a coincidence of signals from several $5 \times 5 \text{ cm}^2$ plastic scintillation counters and anode signals from the MWPCs to ensure valid tracking information.

2.4 Readout electronics

For the beam test, a new read-out system was designed by using analog memory chips. The analog memory chip is based on a chip developed by H. Ikeda [14] for a cosmic-ray experiment. We borrowed the chips from NASDA (National Space Development Agency of Japan), and developed the chip control system. In the analog memory chip, the signals of 32 channels are preamplified, sampled in $1 \mu\text{s}$ intervals, and stored in an 8 steps deep analog pipeline. Figure 4 shows a schematic view of the readout system with these analog memories. Two 32 channel analog memories are attached to each 64 channel PMT. The memories corresponding to four PMTs are controlled by a 256 channel memory controller. When the gate pulse is formed from the trigger signal, a control signal is sent from the controller to the analog memories. The difference in the value of the analog memory between the latest and the first memory content is fed to the output. The obtained output values of 256 channels are clocked into one signal train with a period of $10 \mu\text{s}$ per channel. Each analog memory controller outputs the serial signal together with synchronized control signals. These signals are then read by a 12-bit VME ADC (DSP8112, MTT Co.) with a conversion time of $5 \mu\text{s}$.

2.5 Reference RICH

A reference RICH was instrumented with multi-anode PMTs, Hamamatsu R5900-M16, the same photon detector as used in the previous test [10]. The quantum efficiency of the PMTs is around 26% (at 400 nm), and the gain was around $6 \cdot 10^6$ with -900 V applied to the photo-cathode. The PMTs were grouped in a 2×6 array at a 30 mm pitch. Due to a limited number of available PMTs and read-out channels, only a part of the Cherenkov ring was covered with photon detectors.

3 Measurement and results

Most of the test measurements were performed with a π^- beam at $3 \text{ GeV}/c$. To systematically evaluate the detector performance, data were taken with differ-

ent aerogel samples with various transmission lengths and thicknesses. Data were also taken by varying the π^- momentum in the range from 0.5 GeV/ c to 4.0 GeV/ c .

A few typical events are displayed in Figure 5. The hits on PMTs can be associated with the expected position of the Cherenkov ring. The hit near the center of the ring is due to Cherenkov radiation generated by the beam particle in the PMT window. The distribution of accumulated hits is shown in Figure 6. Cherenkov photons from the aerogel radiator are clearly seen with a low background level. The background hit distribution on the photon detector is consistent with the assumption that it originates from Cherenkov photons which were Rayleigh scattered in the radiator.

The pulse-height distribution of the Cherenkov photons detected in one of the flat-panel PMT is shown in Figure 7. The raw data were corrected as follows. A common-mode fluctuation of the base line was subtracted and signals due to cross-talk in the read-out electronics were removed. The signal mainly containing one photoelectron is clearly separated from the pedestal peak. Note, however, that this distribution differs considerably from tube to tube because of the large variation in performance, as described before. For further analysis we also applied a threshold cut to suppress the pedestal noise contribution.

3.1 Cherenkov-angle resolution for single photons

Figure 8(a) shows a typical distribution of the Cherenkov-angle for single photons. The angular resolution was obtained from a fit of this distribution with a Gaussian signal and a linear function for the background. Figure 9 shows the resolution in the Cherenkov angle for the π^- beam at 3 GeV/ c and 20 mm thick aerogel samples. The resolution was around 14 mrad, independent of the refractive index. The main contributions to the resolution of the Cherenkov angle come from the uncertainty in the emission point and from the pixel size of the PMT. The first contribution is estimated to be $\sigma_{emp} = d \sin \theta_c \cos \theta_c / L \sqrt{12}$, where d is the aerogel thickness, θ_c is the Cherenkov angle and L is the distance from an average emission point in the aerogel to the surface of the PMT. The second contribution is $\sigma_{pix} = a \cos^2 \theta_c / L \sqrt{12}$, where a is the pixel size. The measured variation of the resolution with the thickness of aerogel is shown in Figure 10. By comparing the measured resolution and the expected values, we observed a rather good agreement. There was, however, a discrepancy between the two, which can be accounted for by a contribution of about 6 mrad. The discrepancy could arise from the effect of aerogel (non-flat aerogel surface and possible non-uniformities in the refractive index due to position variation and chromatic dispersion), which are subject to further investigation. The uncertainty in the track direction is expected to be negligible at 3 GeV/ c ,

but increases considerably at low momenta (0.5 GeV/ c) due to the effect of multiple-scattering, as can be seen in Figure 11.

3.2 Photoelectron yield

Figure 8(b) shows a typical distribution of the number of hits within $\pm 3\sigma$ from the average Cherenkov angle. The number of hits for the signal region was estimated by subtracting the background from the fits to the Cherenkov-angle distribution. The number of detected photons (N_{pe}) depends on the aerogel thickness and the effect of scattering. It is expressed as

$$N_{pe} = C \int_0^d \int \epsilon(\lambda) \lambda^{-2} \sin^2 \theta_c \exp\left(-\frac{x}{\Lambda(\lambda) \cos \theta_c}\right) d\lambda dx \approx C' \sin^2 \theta_c \Lambda \cos \theta_c \left(1 - \exp\left(-\frac{d}{\Lambda \cos \theta_c}\right)\right),$$

where Λ is the transmission length of the aerogel at an average wave length of 400 nm and $\epsilon(\lambda)$ is quantum efficiency of the PMT. Figure 12 shows the dependence of the number of detected photons on the aerogel thickness. As expected from the above expression, the number of photons does not linearly increase with the aerogel thickness, but saturates due to the scattering effect in aerogel. Figure 13 shows the dependence of the number of photons with transmission length. From the figure the benefit of the improvement in the transmission length of the $n = 1.05$ aerogel from around 15 mm, as used in the previous beam test, to 45 mm using the new production technique becomes evident. The dependence on the pion momentum, displayed in Figure 14, is fitted with the form expected from the Cherenkov relations, and shows a good agreement. For pions with momenta above 1 GeV/ c , the number of detected Cherenkov photons was typically around 6 for aerogel samples with $n = 1.05$.

The performance of the RICH counter under study was compared in the same set-up with the performance of the reference counter with a well-known photon detector, Hamamatsu R5900-M16 multi-anode PMTs. Since the two counters have a different active area fraction (84% for the flat-panel PMTs, and 36% for the R5900-M16 PMTs) and a different acceptance, the comparison of the photon yields was made by normalizing to the full active surface. While the flat-panel yield for a particular case was 6.2, which resulted in 7.8 if extrapolated to the full active area, the corresponding number for the R5900-M16 was 12. It appears that this difference is mainly due to the rather low quantum efficiency and amplification of some of the flat-panel tubes employed. This, in turn, causes inefficiencies in single photon detection with a given threshold. If the best tube in the set is normalized to the full acceptance, the corresponding number increases to 10, and we would expect about 8 photons per ring.

3.3 Particle Identification

Finally, we estimate the performance of pion/kaon separation in the momentum range of around 4 GeV/ c , which is of considerable importance for the Belle experiment. If we take into account a typical measured value for the single-photon angular resolution, $\sigma_c \sim 14$ mrad, and the number of detected photons $N_{pe} \sim 6$, typical for 20 mm thick aerogel samples with $n = 1.05$, we can estimate the Cherenkov angle resolution per track to be $\sigma_c/\sqrt{N_{pe}} = 5.7$ mrad. This naive estimate is also confirmed by the direct measurement shown in Figure 15. Here, the track-by-track Cherenkov angle is calculated by taking the average of the angles measured for hits around the predicted position of the Cherenkov ring. From this we can deduce that at 4 GeV/ c , where the difference of Cherenkov angles for pions and kaons is 23 mrad, a 4σ separation between the two is possible. As an additional cross check, we have also collected data with the pion beam of 1.1 GeV/ c , which can be used to represent a kaon beam of 4 GeV/ c (apart from a slightly larger sigma due to multiple scattering). As can be seen from Figure 15, the two peaks are well separated. Thus, the proximity focusing aerogel RICH seems to be promising for the upgrade of the Belle PID system at the forward region.

4 Conclusions

We report on the test beam results of a proximity focusing RICH using aerogel as the radiator. To obtain larger photoelectron yields, we used flat-panel multi-anode PMT with a large effective area, and aerogel samples produced with a recently developed method which have a higher transmission length than before. We also developed a multi-channel PMT read-out system using analog memory chips. A clear Cherenkov ring from the aerogel radiator could be observed, and the number of photons was enhanced compared to that in previous tests. We performed a systematic study of the detector using various samples of the aerogel. The typical angular resolution was around 14 mrad and the number of detected photoelectrons was around 6. The pion/kaon separation at 4 GeV/ c is expected to be around 4σ .

However, we still have some issues which have to be solved for implementation in the Belle spectrometer. The most important item is the development of a PMT which can be operated under a strong magnetic field (1.5T). An example of a candidate for such a device is a multi-anode hybrid photodiode (HPD) or hybrid avalanche photodiode (HAPD). Of course, for a good candidate, its ability to efficiently detect single photons on a large active area has to be demonstrated. The other item is mass production of the aerogel tiles. While we have demonstrated that the new production method significantly increases

the transmission length of the $n = 1.05$ aerogel, the production method has to be adapted to stable good-quality manufacturing. We will study these items at the next stage towards construction of a real detector.

5 Acknowledgment

We would like to thank the KEK-PS members for operation of accelerator and for providing the beam to the π^2 beam line. We also thank H. Ikeda (KEK) and the Meisei Co. for their help in preparing the read-out electronics, the Matsushita Electric Works Ltd. for the good collaboration in developing the new aerogel type, and Hamamatsu Photonics K.K. for their support in equipping the photon detector. We also thank A.Bondar (BINP, Novosibirsk) for providing us excellent aerogel samples, and Dr. T.Goka of NASDA for providing us their read-out chips. One of the authors (T.M.) is grateful to Fellowships of the Japan Society for the Promotion of Science (JSPS) for Young Scientists. This work was supported in part by a Grand-in-Aid for Scientific Research from JSPS and the Ministry of Education, Culture, Sports, Science and Technology under Grant No. 13640306, 14046223, 14046224, and in part by the Ministry of Education, Science and Sports of the Republic of Slovenia.

References

- [1] M.Cantin et al. Nucl. Instr. Meth. **118** (1974) 177-182
- [2] A.Abashian et al., Nucl. Instr. and Meth. A **479** (2002) 117
- [3] T.Sumiyoshi et al., Nucl. Instr. and Meth. A **433** (1999) 385-391
- [4] T.Iijima et al., Nucl. Instr. and Meth. A **453** (2000) 321
- [5] I. Adachi et al., Nucl. Instr. and Meth. A **355** (1995) 390; T. Sumiyoshi et al., J. Non-Cryst. Solids **225** (1998) 369
- [6] D.E.Fields et al. Nucl. Instr. Meth. A **349**(1994) 431-437; R. De Leo et al., Nucl. Instr. and Meth. A **401** (1997) 187
- [7] N.Akopov et al. Nucl. Instr. Meth. A **479** (2002) 511-530
- [8] T.Ypsilantis and J.Seguinot, Nucl. Instr. Meth. A **368** (1995) 229-233
- [9] T.Iijima, "Aerogel Cherenkov Counter in Imaging Mode", JPS Meeting, Tokyo Metropolitan University, September 1997.

- [10] I. Adachi et al., "Test of a proximity focusing RICH with aerogel as radiator", Proceedings for the IEEE Nuclear Science Symposium, Norfolk, VA, November 10-15, 2002, Trans. Nucl. Sci. 50 (2003) 1142, hep-ex/0303038, ; T.Iijima et al., Nucl. Instr. Meth. A **502**(2003) 231-235
- [11] Hamamatsu Photonics K.K.
- [12] Matsushita Electric Works Ltd. has a Japanese patent (No. 2659155) for usage of DMF as solvent to make aerogel.
- [13] A.R. Buzykaev et al. Nucl. Instr. Meth. A **433** (1999) 396-400
- [14] H.Ikeda et al. Nucl. Instr. Meth. A **372** (1996) 125-134



Fig. 1. Photon detector, an array of 16 H8500 PMTs, mounted at a 52.5 mm pitch.

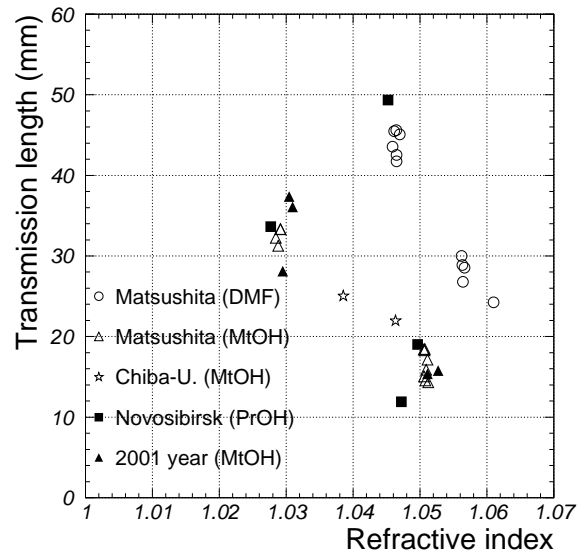


Fig. 2. Transmission length at 400 nm and refractive index at 405 nm for the aerogel samples used in the test.

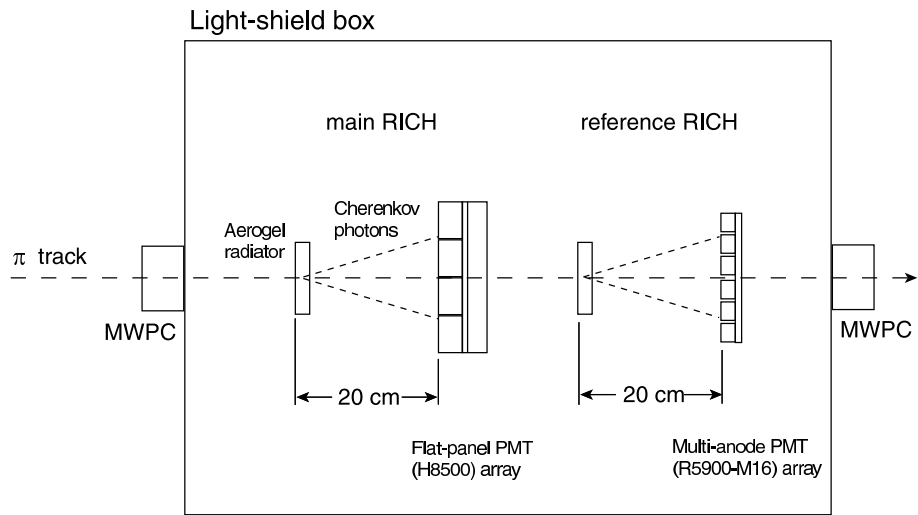


Fig. 3. Experimental set-up.

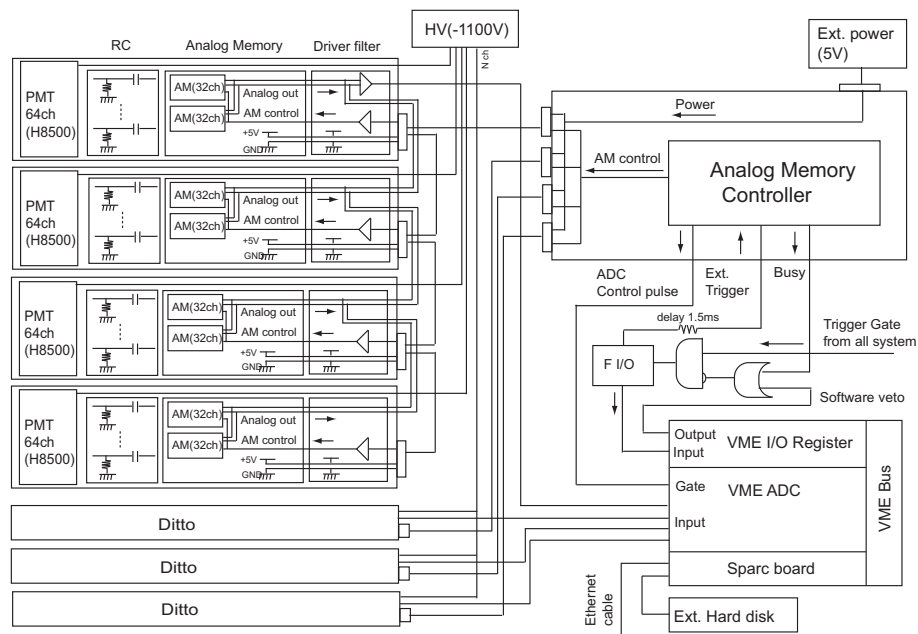


Fig. 4. Schematics of the read-out system for the flat-panel PMTs.

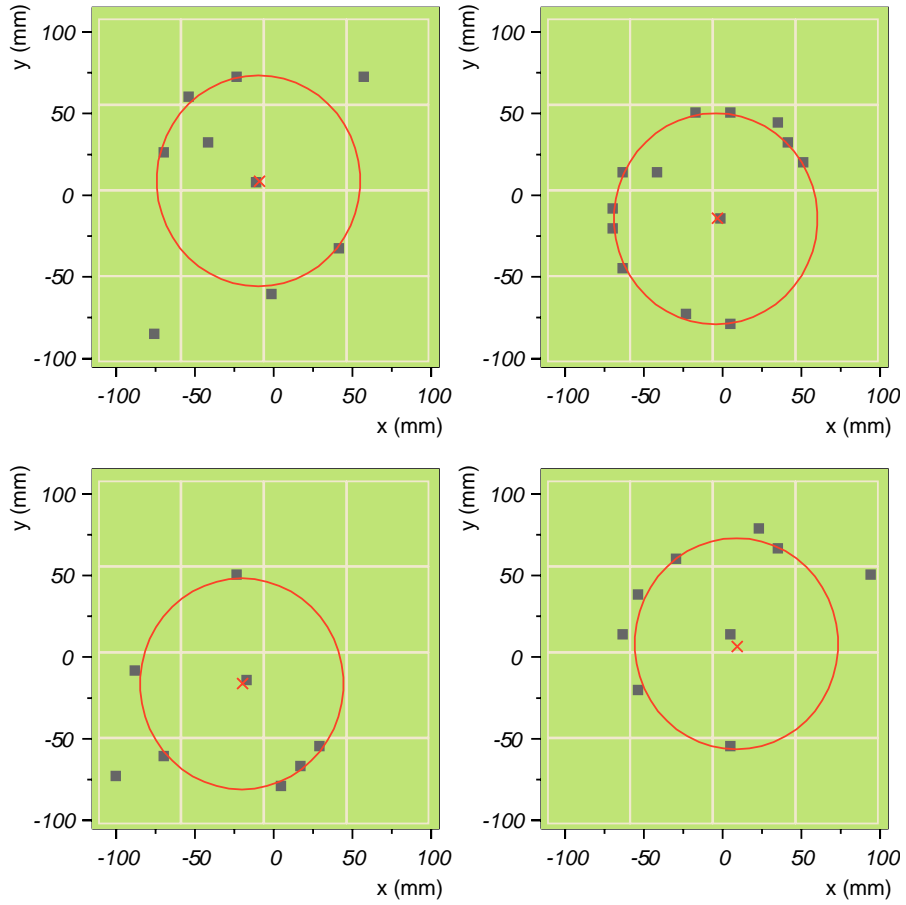


Fig. 5. Some examples of event hit patterns for 3 GeV/ c pions. The circle corresponds to the Cherenkov ring as expected from the measured beam particle track. The dot corresponds to the impact point of the track upon the PMT window.

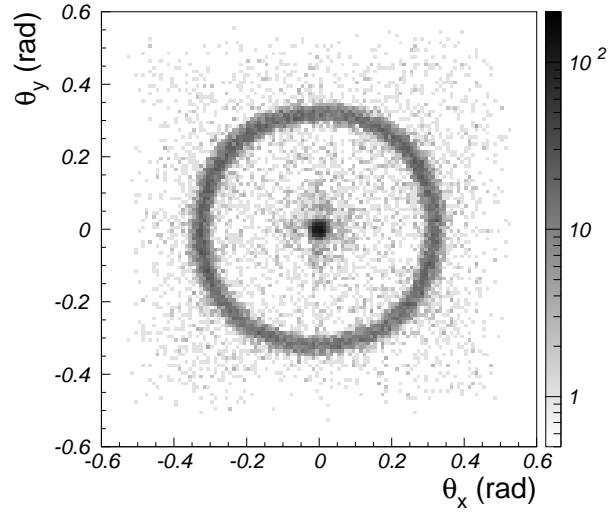


Fig. 6. Distribution of PMT hits in the Cherenkov x, y space for 3 GeV/ c pions.

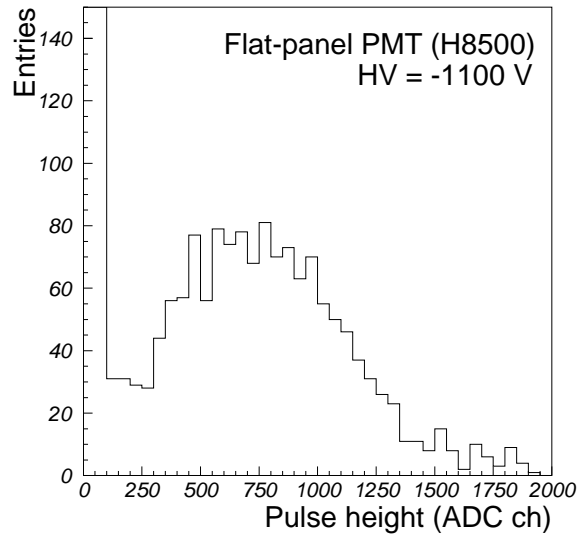


Fig. 7. Pulse-height distribution for the flat-panel PMT (H8500) for the hits in the region within 3σ of the mean Cherenkov angle. Data were corrected with the procedure described in the text. In this figure, the pulse-height distribution for the high sensitive PMT is shown. For further analysis, we used the hits above a threshold ADC value, 120.

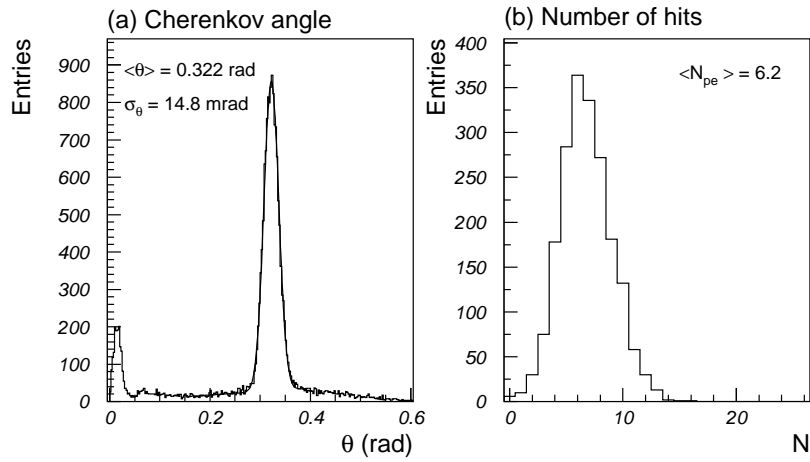


Fig. 8. Distribution over the Cherenkov angle for single photons (a), and the number of detected photons per ring (b), for a 20 mm thick aerogel radiator sample with $n = 1.056$ and a transmission length of 30 mm.

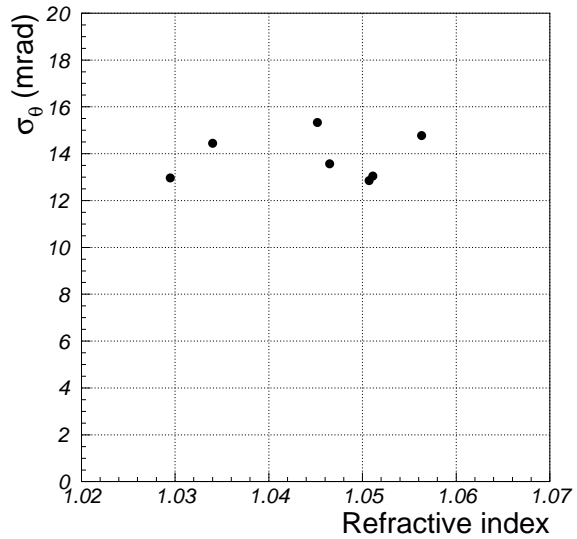


Fig. 9. Typical single photon resolution for 20 mm thick aerogel samples.

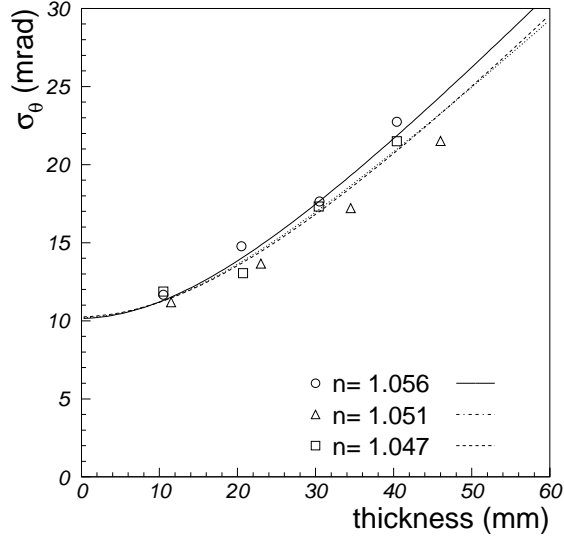


Fig. 10. Angular resolution as a function of the aerogel thickness. The symbols correspond to the data for the different samples and the curves are function described in the text (also including the unknown contribution of about 6 mrad).

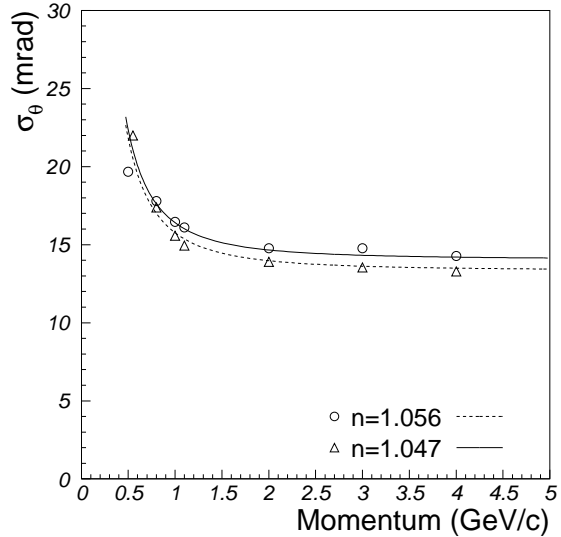


Fig. 11. Angular resolution as a function of the charged particle momentum for two different samples. The symbols correspond to the data and the curves are fits including the effect of multiple-scattering.

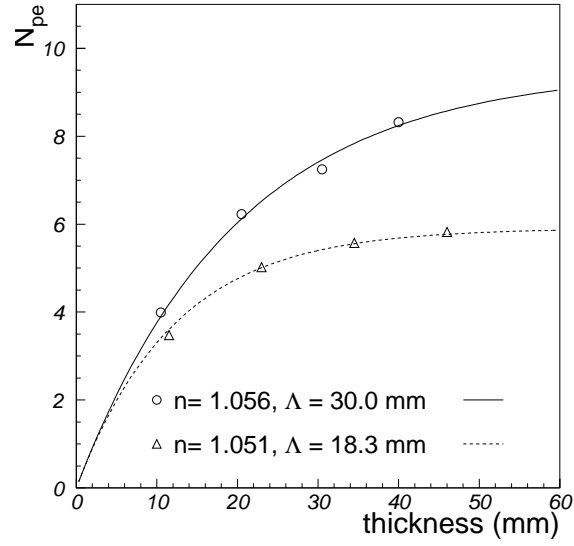


Fig. 12. Number of detected photons per Cherenkov ring as a function of the aerogel thickness. The symbols correspond to the data and the curves are fits described in the text.

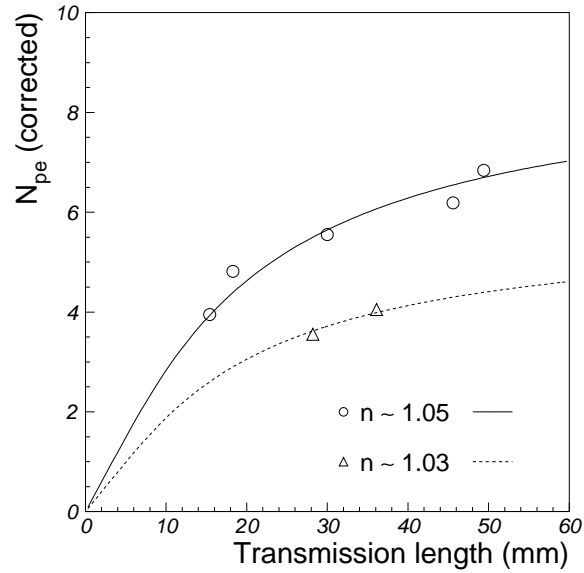


Fig. 13. Number of detected photons per Cherenkov ring (N_{pe}) for 20 mm thick aerogel samples as a function of the transmission length. N_{pe} is corrected for the refractive index to $n = 1.05$ and $n = 1.03$ respectively. The symbols correspond to the data and the curves are fits described in the text.

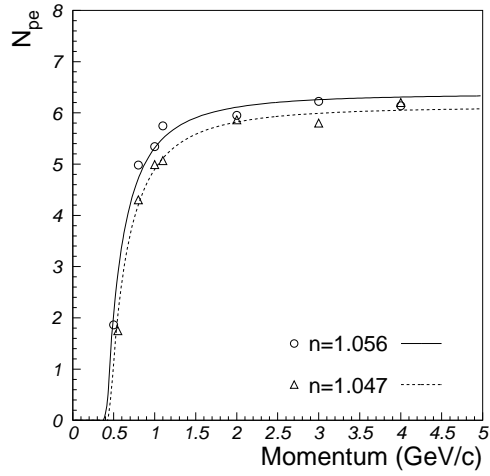


Fig. 14. Number of detected photons per Cherenkov ring as a function of the charged particle momentum. The symbols correspond to the data and the curves are fits described in the text.

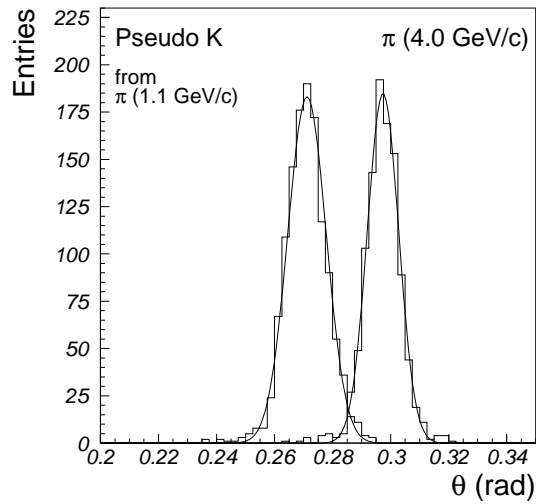


Fig. 15. Cherenkov angle per track for pions of 4.0 GeV/c and 1.1 GeV/c. Pions at 1.1 GeV/c are used to represent the kaon beam of 4 GeV/c. The angular resolutions for 4.0 GeV/c and 1.1 GeV/c are 5.4 mrad and 6.7 mrad and two peaks are separated by 4.2σ .